



HAL
open science

Nano-sculptured vanadium oxide thin films for benzene detection

Jean-Baptiste Sanchez, Anna Krystianiak, Emmanuel Dordor, Olivier Heintz, Nicolas Geoffroy, Nicolas Martin

► **To cite this version:**

Jean-Baptiste Sanchez, Anna Krystianiak, Emmanuel Dordor, Olivier Heintz, Nicolas Geoffroy, et al.. Nano-sculptured vanadium oxide thin films for benzene detection. *Materials Letters*, 2024, 371, pp.136937. hal-04745703

HAL Id: hal-04745703

<https://hal.science/hal-04745703v1>

Submitted on 21 Oct 2024

HAL is a multi-disciplinary open access archive for the deposit and dissemination of scientific research documents, whether they are published or not. The documents may come from teaching and research institutions in France or abroad, or from public or private research centers.

L'archive ouverte pluridisciplinaire **HAL**, est destinée au dépôt et à la diffusion de documents scientifiques de niveau recherche, publiés ou non, émanant des établissements d'enseignement et de recherche français ou étrangers, des laboratoires publics ou privés.

Nano-sculptured vanadium oxide thin films for benzene detection

Jean-Baptiste Sanchez^{a,*}, Anna Krystianiak^b, Emmanuel Dordor^a, Olivier Heintz^b, Nicolas Geoffroy^b, Nicolas Martin^a

^a Université de Franche-Comté, CNRS, institut FEMTO-ST, F-25000 Besançon, France

^b Laboratoire ICB, UMR 6303 CNRS, Univ. Bourgogne, 9, Avenue Alain Savary, BP 47 870, 21078 Dijon Cedex, France

Abstract: DC magnetron sputtering was used to prepare nano-sculptured vanadium oxide thin films and their gas sensing properties were investigated for the detection of benzene traces in the air. Oblique nanostructures showed excellent responses to benzene, as well as good repeatability and stability, which makes it a very reliable sensor for the detection of very low concentrations of benzene (a few ten ppbs) in air and under realistic conditions of humidity, as high as 60% RH at 25°C.

Keywords: GLAD sputtering, benzene, vanadium oxide, gas sensor

1. Introduction

Prolonged inhalation of benzene, even at minimal concentrations, can gradually contribute to the development of various diseases such as aplastic anemia, leukemia, and multiple myeloma, both in the short and long term [1]. The major sources of benzene exposure are automobile service stations, tobacco smoke, exhaust from motor vehicles, and industrial emissions. Real time and *in situ* identification of this toxic compound in the air is challenging and today the only devices available for monitoring benzene including gas chromatography-mass spectroscopy systems [2], Fourier transform infrared (FTIR) single-beam spectrophotometer [3] or photoionization detectors [4] are very expensive and deployment for *in situ* analysis is an issue. Metal oxide semiconductors (MOS) gas sensors are very promising for this particular application as they are sensitive to a wide range of chemical species, small in size, easy to use and highly flexible in the manufacturing process. Among the most studied metal oxides, tin and tungsten oxides have shown their ability to detect toxic compounds including benzene [5]. Besides its chemical and thermal stability, vanadium pentoxide (V_2O_5) exhibits very interesting electronic and optical properties. This compound has already been extensively studied for the development of photodetectors [6], UV sensors [7], gasochromic sensors [8] and so on. It is only in recent years that vanadium oxides have attracted the attention of researchers for gas sensing application [9]. Regarding benzene detection,

existing literature only notes the use of V_2O_5 as a dopant in SnO_2 -based gas sensors [10]. The present work focuses on the elaboration of miniaturized gas sensors based on pure V_2O_5 using conventional and Glancing Angle Deposition (GLAD) sputtering methods for the detection of benzene in the air. Research has already demonstrated that GLAD method is a highly promising technique for the development of MOS gas sensors. This is due to its ability to precisely control the growth and architecture of the film, even at the nanoscale [11, 12]. Here, we compare and discuss the sensing performances of both sensors tested in the same conditions and under realistic relative humidity.

2. Experimental section

DC magnetron sputtering was used to deposit vanadium oxide thin films. Vanadium metallic target (purity of 99.9 %, 51 mm diameter) was dc sputtered using a current $I = 200$ mA. Oxygen to argon flow rate ratio was fixed at 0.6, leading to a total sputtering pressure of 0.3 Pa. Vanadium oxide films were simultaneously deposited onto (100) silicon substrates and interdigitated electrodes equipped with micro-hotplate at two different deposition angles ($\alpha = 0^\circ$ and 80° for conventional and GLAD films, respectively). The deposition time was adjusted to get a film thickness close to 200 nm. Films produced on silicon were used for physicochemical characterization (XRD, XPS) while those elaborated onto interdigitated micro-electrodes were used for examining morphology of films and sensing tests. A specially designed shadow mask was employed to selectively deposit materials onto interdigitated micro-electrodes, resulting in a sensitive area of approximately 0.02 mm^2 . Sensing tests were performed under various concentrations of benzene in nearly dry air (8% RH at 25°C) and under realistic conditions of relative humidity, as high as 60% RH at 25°C . Further details on the deposition and sensing procedure are in [12].

3. Results and discussion

Fig. 1 reveals the top view morphology of vanadium oxide films sputtered onto interdigitated electrodes with two distinct angles, as-deposited and after the annealing treatment at 500°C for 24 hours. For film prepared with conventional sputtering method ($\alpha = 0^\circ$), we observe well-defined individual rounded nanostructures (size < 500 nm) with vertical orientation. After annealing treatment, the morphology is preserved with an increase in size ($\sim 1 \mu\text{m}$). By depositing at an oblique angle ($\alpha = 80^\circ$), individual striated and more regular nanostructures appear in the direction of the incoming atomic flux.

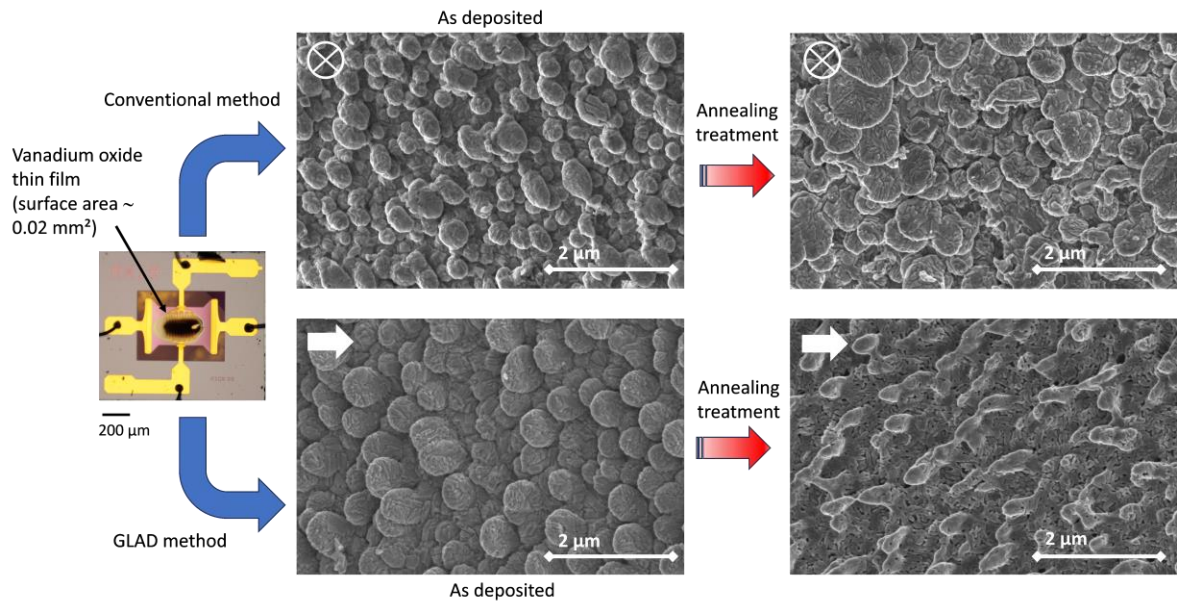


Fig. 1: miniaturized vanadium oxide-based gas sensor and micrographs of sensitive films for conventional and GLAD method. Arrows indicate the incoming flux of particles.

The morphology significantly changes with the annealing treatment, where nanostructures coalesce to form a highly porous and inhomogeneous film with some oriented structures. We have already demonstrated that high porosity will likely result in outstanding LOD [12]. To further understand the influence of annealing treatment on the crystallographic properties of vanadium oxide films, XRD was performed on as deposited materials and after a thermal treatment of 250°C and 500°C in air.

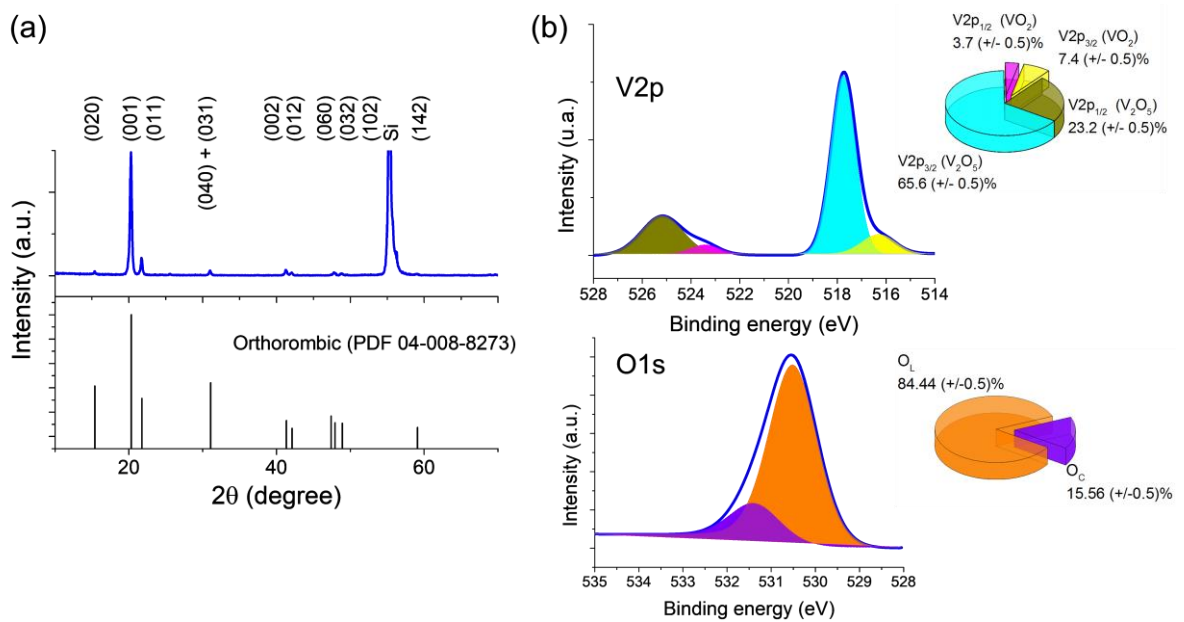


Fig. 2: (a) XRD patterns and (b) XPS high resolution spectra of V2p and O1s for conventional ($\alpha = 0^\circ$) vanadium oxide thin film annealed at 500°C.

As-deposited thin films remain amorphous without crystallinity (Fig. S1 (a)). By increasing the annealing treatment up to 500 °C (Fig. 2 (a) and S1 (a)), XRD pattern reveals several diffraction peaks between 10° and 70° which are assigned to the α -V₂O₅ phase (orthorhombic, JCPDS Card no.41-1426, space group Pmmn (59)). The average crystallite size is estimated at 150±5 nm and the significant relative peak intensities suggest a strong preferential orientation. The effect of the annealing treatment on the chemical bonding states of both materials was also investigated using XPS technique (Fig. 2 (b) and S1 (b)). All films exhibited similar surface chemistry, with no contamination. The decomposition of V2p_{3/2} and V2p_{1/2} peaks indicates that thin films are essentially built-up of V₂O₅ and VO₂ but the contribution of vanadium dioxide decreases drastically when increasing temperature. The O1s spectrum shows that lattice oxygen species (O_L) corresponding to O²⁻ ions connected to metal cations are dominant compared to the chemisorbed oxygen species (O_C). It is well established that these chemisorbed species contribute to the overall detection mechanism, and thus their quantity is directly linked to the gas sensor's detection performance [12]. Figure S1 demonstrates that the annealing treatment increases the amount of O_C, indicating enhanced sensing capabilities. The electrical response of MOS-based gas sensors is significantly affected by their operating temperature. Fig. 3 (a) plots the variation of the normalized conductance of both sensors for different sensing temperatures and under 313±4 ppb of benzene for 3 min in nearly dry air (8% RH at 25°C). The optimized temperatures are 400 and 450°C for conventional and GLAD sensors, respectively. The GLAD sensor shows much higher response compared to the conventional one. Fig. 3 (b) depicts a sequence of real time responses of both sensors at their respective operating temperature and under various benzene concentrations, randomly selected. Each concentration was replicated at least three times. For both sensors, the limit of detection (LOD) was estimated to 28±4 ppb, which is two order of magnitude lower than the occupational standards for benzene air concentrations (~ 1 ppm) [13]. For both sensors, the normalized conductance gradually increases with the benzene concentration (Fig. 3 (c)). Nevertheless, it is important to highlight that the conventional sensor reaches a smooth plateau for concentrations above 100 ppb more quickly than the GLAD sensor. This is attributed to the rapid saturation of the less porous sensitive layer obtained by conventional sputtering when increasing benzene concentrations. To complete sensing tests, influence of relative humidity was also studied. Figure 3 (d) illustrates the real-time normalized conductance of conventional and GLAD sensors to different benzene concentrations under 30% and 60% RH at 25°C, which reflects typical indoor air humidity levels.

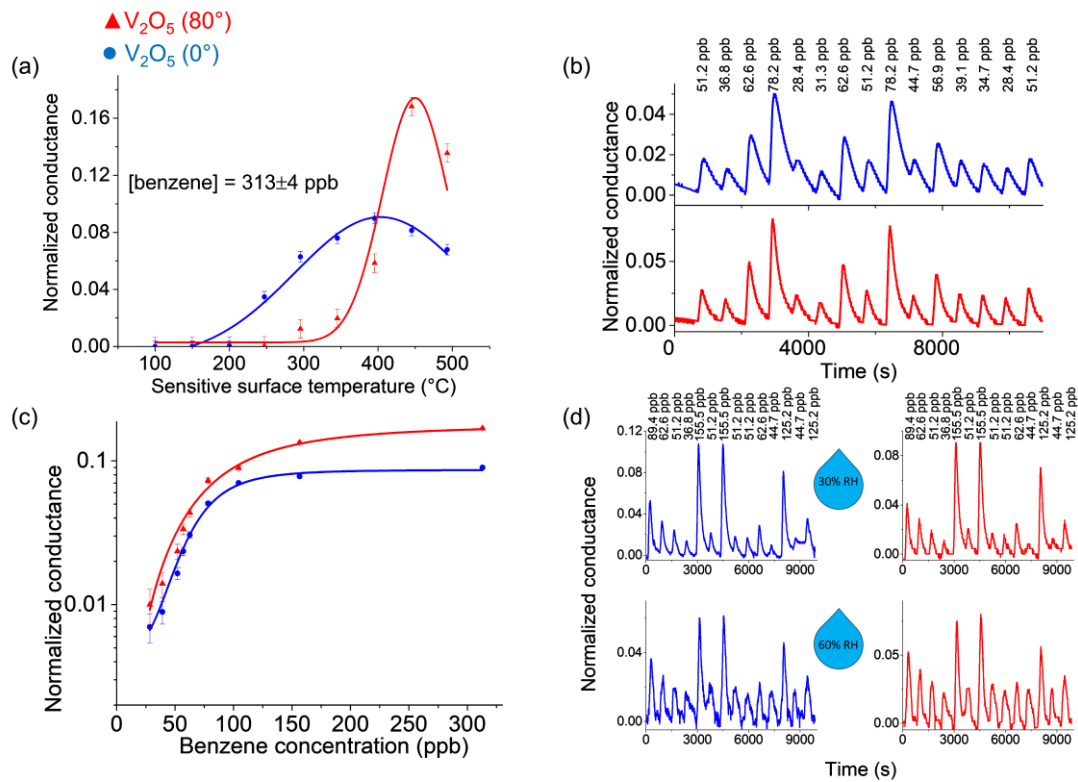


Fig.3: (a) Evolution of the normalized response as a function of the sensitive surface temperature. (b) Real-time response for various benzene concentrations. (c) Normalized response as a function of the benzene concentration. (d) Real-time response for various benzene concentrations under 30% and 60% RH at $25^{\circ}C$.

It is noteworthy that the presence of humidity slightly affects the sensing response of both sensors, with much noise for the conventional sensor although electric signals are still repeatable. The LOD is now estimated to 36 ± 4 ppb for both sensors.

Table 1: Non-exhaustive list of various types of metal oxide-based sensors for the detection of benzene.

Material	Sensing temperature ($^{\circ}C$)	LOD of benzene (ppm) / (t_{res}/t_{rec}) (s)	Refs.
Nano-sculptured V_2O_5	450	0.028 (75/115)	This work
Ordered SnO_2 nanorods arrays	450	10 (1.5/-)	[5]
Raisin($Pd-Co_3O_4$)-bread(SnO_2) structure	325	5 (-/-)	[14]
$Pd-SnO_2$ NPs	400	1 (15/15)	[15]
WO_3 nanosheets	320	50 (36/38)	[16]

For the sake of comparison, Table 1 reports on the most relevant metal oxide-based gas sensors for the detection of benzene. We notice that nano-sculptured vanadium oxide sensors exhibit better LOD than previously reported MOS gas sensors, even under realistic conditions of humidity.

4. Conclusion

DC magnetron sputtering followed with an annealing treatment produced nano-sculptured vanadium oxide thin films for the detection of benzene traces. Both deposition methods conduct to benzene sensors with high sensitivity, stability and repeatability, but the well-developed porosity associated to the GLAD method allows enhanced sensing performances of V₂O₅ thin films, even with high level of relative humidity.

CRedit authorship contribution statement

J.-B. Sanchez: Conceptualization, Investigation, Supervision, Writing – original draft. A. Krystianiak, E. Dordor, O. Heintz, N. Geoffroy: Investigation, Nicolas Martin: Investigation, Writing - Review & Editing.

Declaration of competing interest

The authors declare no conflict of interest.

Acknowledgements

This work was partially supported by the French RENATECH network and its FEMTO-ST technological facility. This work has been achieved in the frame of the EIPHI Graduate school (contract "ANR-17-EURE-0002").

Appendix A. Supplementary data

Supplementary data to this article can be found online at:

Reference

- [1] A. Yardley-Jones, D. Anderson, D. V. Parke, Br. J. Ind. Med. 48 (1991) 437-44.
<https://doi.org/10.1136/oem.48.7.437>.

- [2] S. Narayan Sinha, P.K. Kulkarni, N.M. Desai, S.H. Shah, G.M. Patel, M.M. Mansuri, D.J. Parikh, H.N. Saiyed, *J. Chromatogr. A*, 1065 (2005) 315–319. <https://doi.org/10.1016/j.chroma.2004.12.070>.
- [3] J. Jeffers, C. Roller, K. Namjou, M. Evans, L. McSpadden, J. Grego, P. McCann, *Anal. Chem.* 76 (2003) 424–432. <https://doi.org/10.1021/ac0345392>.
- [4] G. Coelho Rezende, S. Le Calvé, J. J. Brandner, David Newport, *Sens. Actuators B Chem.*, 287 (2019) 86–94. <https://doi.org/10.1016/j.snb.2019.01.072>.
- [5] J. Lee, H. Min, Y.-S. Choe, Y. Gyu Lee, K. Kim, H.-S. Lee, W. Lee, *Sens. Actuators B Chem.*, 394, (2023) 134359. <https://doi.org/10.1016/j.snb.2023.134359>.
- [6] S. Wang, L. Wu, H. Zhang, Z. Wang, Q. Qin, X. Wang, Y. Lu, L. Li, M. Li, *Materials* 15 (2022) 8313. <https://doi.org/10.3390/ma15238313>.
- [7] K. Daeil, Y. Junyeong, L. Geumbee, H. Jeong Sook, *Nanoscale*, 6 (2014) 12034–12041. <https://doi.org/10.1039/C4NR04138K>.
- [8] C.L. Chen, C.L. Dong, Y.K. Ho, C.C. Chang, D.H. Wei, T.C. Chan, J.L. Chen, W.L. Jang, C.C. Hsu, K. Kumar, *Europhys. Lett.* 101 (2013) 17006. <https://doi.org/10.1209/0295-5075/101/17006>.
- [9] R. Alammouza, M. Lazerges, J. Pironon, I. Bin Taher, A. Randi, Y. Halfaya, S. Gautier, *Sens. Actuators A Phys.*, 332 (2021) 113179. <https://doi.org/10.1016/j.sna.2021.113179>.
- [10] C. Feng, X. Li, C. Wang, Y. Sun, J. Zheng, G. Lu, *RSC Adv.* (2014) 4, 47549. <https://doi.org/10.1039/c4ra06120a>.
- [11] P. Luo, M. Xie, J. Luo, H. Kan, Q. Wei, *RSC Adv.*, 10 (2020) 14877, <https://doi.org/10.1039/d0ra00488j>.
- [12] A. El Mohajir, M. Arab Pour Yazdi, A. Krystianiak, O. Heintz, N. Martin, F. Berger, J.-B. Sanchez, *Chemosensors* 10 (10) (2022) 426. <https://doi.org/10.3390/chemosensors10100426>.
- [13] C. P. Weisel, *Chem. Biol. Interact.*, 184 (2010) 58–66. <https://doi.org/10.1016/j.cbi.2009.12.030>.
- [14] K. Beom Kim, Y. Kook Moon, T.-H. Kim, B.-H. Yu, H.-Y. Li, Y. Chan Kang, J.-W. Yoon, *Sens. Actuators B Chem.*, 386 (2023) 133750. <https://doi.org/10.1016/j.snb.2023.133750>.

[15] J.-H. Kim, P. Wu, H. Woo Kim, S. Sub, ACS Appl. Mater. Interfaces 8 11 (2016) 7173–7183. [https://doi:10.1021/acsami.6b01116](https://doi.org/10.1021/acsami.6b01116).

[16] D. Zhang, Y. Fan, G. Li, Z. Ma, X. Wang, Z. Cheng, J. Xu, Sens. Actuators B: Chem., 293 (2019), 23-30. <https://doi.org/10.1016/j.snb.2019.04.110>.